LUND UNIVERSITY

Zero-phonon linewidth and phonon satellites in the optical absorption of nanowire-based quantum dots

Lindwall, Greta; Wacker, Andreas; Weber, Carsten; Knorr, Andreas

Link to publication

Zero-Phonon Linewidth and Phonon Satellites in the Optical Absorption of Nanowire-Based Quantum Dots

Greta Lindwall[*] and Andreas Wacker[†]

Mathematical Physics, Lund University, Box 118, 22100 Lund, Sweden

Carsten Weber and Andreas Knorr

Institut für Theoretische Physik, Technische Universität Berlin, Hardenbergstr. 36, 10623 Berlin, Germany
(Received 2 March 2007; published 21 August 2007)

The optical properties of quantum dots embedded in a catalytically grown semiconductor nanowire are studied theoretically. In comparison to dots in a bulk environment, the excitonic absorption is strongly modified by the one-dimensional character of the nanowire phonon spectrum. In addition to pronounced satellite peaks due to phonon-assisted absorption, we find a finite width of the zero-phonon line already in the lowest-order calculation.

Decoherence in semiconductor heterostructures such as quantum dots are of central importance due to their use in advanced photonic structures such as emitters of single and entangled photons [1,2] for quantum cryptography and in photonic crystals for solid state cavity QED [3]. In particular, the stochastic modulation of the phase by a bath via electron-phonon scattering constitutes an important source of optical decoherence. In this Letter, we show that the dimensionality of the semiconductor structure embedding the quantum dot essentially affects the dephasing properties.

Catalytically grown semiconductor nanowires [4] allow for the inclusion of quantum dots which exhibit a zero-dimensional density of states as probed by conductance measurements [5,6]. Here, we focus on the optical absorption line shape of the transition between the highest valence-band state and the lowest conduction-band state within the quantum dot (the lowest quantum confined interband transition in the dot), where a clear signal from the bound exciton can be observed in the photoluminescence spectrum [7]. Intensive single-photon emission was demonstrated suggesting potential applications in quantum information processing of nanowire-based quantum dots [8].

The optical absorption of electromagnetic radiation by this two-level transition is mediated via a coherent superposition of the initial and final state, the polarization. The temporal coherence decay of the polarization (dephasing time) is directly reflected in the line shape of the optical absorption as a function of frequency. For quantum dots, the discreteness of energy levels does not allow for standard scattering transitions known from bulk material, where the phonon energy matches the energy difference between initial and final states. Thus, long dephasing times of several hundred picoseconds have been observed [9] in a sample of self-organized quantum dots [10]. In addition, calculations for such structures show that scattering of electrons with phonons of the embedding material leads

to sidebands in the excitonic spectra which are due to phonon-assisted processes occurring on a shorter time scale [11–15], features which have also been observed experimentally [9,16,17]. The width of the central absorption peak itself, the zero-phonon line, is an issue of particular interest, as standard approaches such as the independent Boson model [11,18–20] provide a zero width in contrast to the experimental findings [9,21]. These works focused on quantum dots embedded in a bulk system as appropriate for the self-organized dots addressed in the experiment [9]. In addition, etched mesas with small diameters down to the 200 nm range have been studied, where the change in zero-phonon linewidth was attributed to phonon scattering at the etched walls [22,23].

In contrast, we are focusing here on dots embedded in catalytically grown nanowires with a diameter in the 50 nm range. These wires have a very regular structure [24], and thus we expect significantly longer lifetimes for the quasi one-dimensional phonon modes. We show that the dimensionality of the phonon spectrum essentially modifies the optical absorption of the embedded quantum dot. In particular, for nanowire-based quantum dots, a finite width of the zero-phonon line is found within the independent Boson model.

We approximate the hexagonal GaAs nanowires [25] to be cylindrical with a radius of 25 nm and evaluate the phonon spectrum for the nanowires within an isotropic continuum model following Ref. [26]. This geometry results in a classification of the phonon modes by a one-dimensional Bloch vector q and a multitude of modes numbered by κ with increasing energy. The resulting dispersion $\omega_{q\kappa}$ is shown in Fig. 1, where we restricted to the compressional modes, as only those couple via the electron-phonon deformation potential interaction to the radially symmetric electron states considered below.

Several modes of the phonon spectrum are shown in Fig. 2. Modes 1, 2, 4, and 6 are essentially axial modes, where the elongation is parallel to the wire, while modes 3
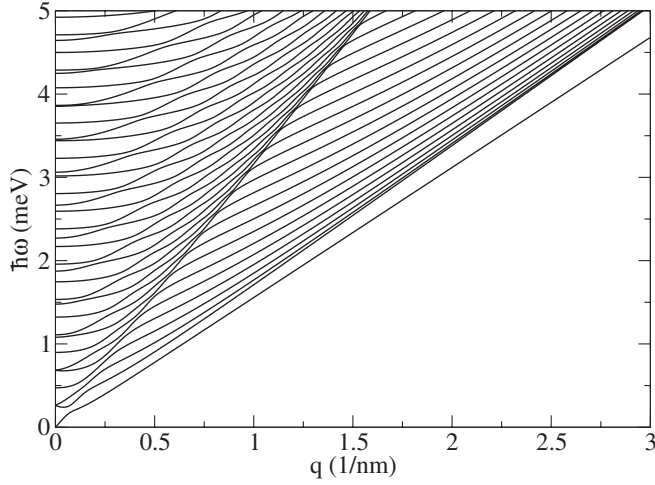
FIG. 1. Dispersion relation $\hbar\omega_{q\kappa}$ for the acoustic phonons in a cylindrical GaAs nanowire with a radius of 25 nm. (Parameters: mass density $\rho = 5370$ kg/m^3, longitudinal sound velocity $v_L = 4780$ m/s, transverse sound velocity $v_T = 2560$ m/s). Only the compressional modes are shown.

and 5 exhibit a significant radial part as well. For a finite wave vector, both types mix, which is of particular relevance for modes 2 and 3, as well as 5 and 6, which are degenerate at $q = 0$.

We calculate the absorption from the independent Boson model following Refs. [11,18–20,27]. For a δ-shaped laser pulse applied at $t = 0$, the polarization $p(t)$ between the electron and hole evolves as

$$p(t) = p(0)e^{-i\omega_{\text{ren}}t}\exp\left[-\sum_{q\kappa}\frac{|g_x^{q\kappa}|^2}{\hbar^2\omega_{q\kappa}^2}\left(4n_{q\kappa}\sin^2\frac{\omega_{q\kappa}t}{2}\right.\right.$$

$$\left.\left. + 1 - e^{-i\omega_{q\kappa}t}\right)\right] \quad (1)$$

for $t > 0$, where $n_{q\kappa}$ is the phonon distribution given by the

Bose-Einstein distribution $n_{q\kappa} = (e^{\hbar\omega_{q\kappa}/k_BT} - 1)^{-1}$. The coupling to the phonons renormalizes the transition frequency to

$$\hbar\omega_{\text{ren}} = E_e - E_h - E_{\text{Coulomb}} - \sum_{q\kappa}\frac{|g_x^{q\kappa}|^2}{\hbar\omega_{q\kappa}}, \quad (2)$$

where E_e and E_h are the single-particle electron and hole ground state energy, respectively, and E_{Coulomb} is the exciton binding energy. $\hbar\omega_{\text{ren}}$ is used as the reference point for the frequency detuning in the following absorption spectra. The coupling to the phonons is reflected by the coupling elements

$$g_x^{q\kappa} = \int d^3r[D_c|\Psi_e(\mathbf{r})|^2 - D_v|\Psi_h(\mathbf{r})|^2]\nabla\cdot\mathbf{u}_{q\kappa}(\mathbf{r}) \quad (3)$$

which is the difference between the coupling of the electron and the hole to the respective phonon mode within the deformation potential interaction. We use the interaction parameters $D_c = -14.6$ eV and $D_v = -4.8$ eV for the conduction and valence band, respectively. $\mathbf{u}_{q\kappa}(\mathbf{r})$ is the normalized elongation field of the phonon mode. The wave functions for the electron (e) and hole (h) state are modeled by spherical Gaussian wave functions $\Psi_\alpha(\mathbf{r}) \propto e^{-(r^2+z^2)/2a_\alpha^2}$ with $a_e = 5.8$ nm and $a_h = 3.19$ nm like in Ref. [12]. As the polarization, Eq. (1), is the response to a δ-signal, its Fourier transformation provides the complex susceptibility $\chi(\omega)$ which yields the absorption spectrum via its imaginary part [28].

The resulting absorption spectrum is shown in Fig. 3 both for bulk and wire phonons using identical parameters. For bulk phonons, we find a sharp zero-phonon line, which is here artificially broadened by introducing a finite decay time. This can be motivated by spontaneous recombination
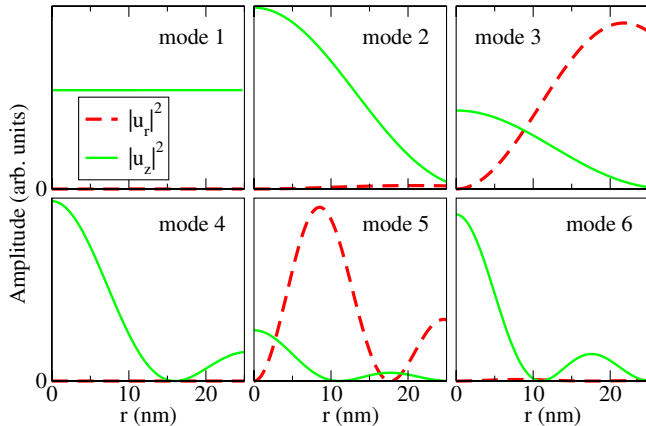

FIG. 2 (color online). Radial (u_r) and axial (u_z) amplitudes as a function of the radial coordinate r for the first six modes of the dispersion relation from Fig. 1. The amplitudes are displayed for $q = 0.003$/nm.
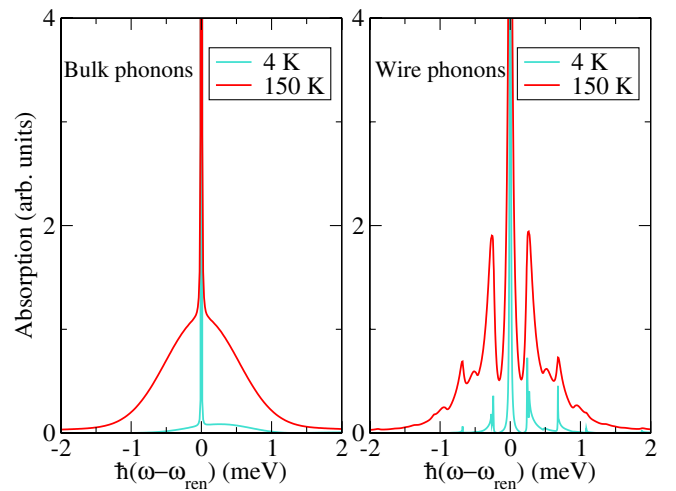

FIG. 3 (color online). Absorption versus detuning from the renormalized transition energy for a spherical quantum dot for different temperatures. Left: bulk phonons (as in Ref. [12]), right: wire phonons from Fig. 1.

or temperature-dependent broadening mechanisms discussed in the literature recently for acoustic [27,29,30] or optical [31,32] phonons. In addition to the zero-phonon line, rather flat absorption features (sidebands) are present for detunings $\hbar|\omega - \omega_{ren}| \lesssim 1$ meV. In contrast, for wire phonons, we find distinct satellite peaks in the sidebands (i) and a finite width of the zero-phonon line without any artificial broadening (ii), which constitute the two central results of this article: (i) Let us first focus on the satellite peaks, which are similar to the result of calculations for a slab-geometry [33]. Figure 4 shows that the peaks in the absorption are related to the extrema in the phonon dispersion. At these extrema, the phonon density of states has singularities. However, not all phonon modes contribute, as their coupling elements differ. For example, the fourth mode is of axial character, i.e., $\mathbf{u}_{q\kappa}(\mathbf{r}) \sim u_0(r)\mathbf{e}_z e^{iqz}$ in cylindrical coordinates (r, z) with the radial and longitudinal coordinates of the wire r and z, respectively, see Fig. 2. Thus, the divergence vanishes with q for $q \to 0$, and so does the corresponding exciton coupling matrix element $g_x^{q\kappa}$, as shown in Fig. 4(c). Thus, this mode couples only weakly to the exciton wave function around its extremum at $q = 0$, and subsequently only a weak peak is observed in the absorption. In contrast, the fifth mode is of radial character leading to a finite exciton coupling matrix element for $q \to 0$ and a strong peak in the absorption. The second phonon mode is of particular interest, as it is of axial nature for $q \to 0$, where the coupling vanishes. However, due to mixing with mode 3 at finite q, its frequency decreases with q for small q, and the minimum of frequency occurs at finite q where its density of states exhibits a singularity. Here, the exciton coupling matrix element is finite so that a strong peak is visible in the absorption. (ii) Now we turn to the broadening of the zero-phonon line: The first phonon mode ($\kappa = 1$) is the only mode which extends to $\omega \to 0$, where it describes a wave of elongations in z direction traveling along the wire:

$$\mathbf{u}_{q1}(\mathbf{r}) \overset{q \to 0}{\sim} N_q\left[\left(1 - \nu\frac{q^2 r^2}{2}\right)\mathbf{e}_z - i\nu qr\mathbf{e}_r + \mathcal{O}(q^3)\right]e^{iqz}, \quad (4)$$

where ν is the Poisson number, which is the ratio between transverse contraction and longitudinal elongation in the direction of the stretching force. In the limit $q \to 0$, it has a linear dispersion $\omega_{q1} = v_1 q$ with $v_1 = \sqrt{E/\rho}$, where E is the Young modulus and ρ the mass density [34]. The proper normalization [18] leads to

$$N_q = \sqrt{\frac{\hbar}{2LA\rho\omega_{q1}}}[1 + \mathcal{O}(q^2 R^2)] \quad (5)$$

with the wire area A and the normalization length L for the phonon modes. Equation (3) yields

$$g_x^{q1} \sim iq\sqrt{\frac{\hbar}{2LA\rho\omega_{q1}}}(D_c - D_v)(1 - 2\nu) \quad \text{for} \quad q \to 0. \quad (6)$$

Furthermore, in thermal equilibrium $n_{q1} \sim k_B T/\hbar\omega_{q1}$ holds for $\omega_{q1} \to 0$. For long times, we evaluate the contribution to the dephasing in the exponential in Eq. (1) analogously to Fermi's golden rule:

$$\frac{4\sin^2\frac{\omega_{q\kappa}t}{2}}{\omega_{q\kappa}^2} \sim 2\pi t\delta(\omega_{q\kappa}).$$

Together, this results in

$$\sum_q \frac{|g_x^{q1}|^2}{\hbar^2\omega_{q1}^2}4n_{q1}\sin^2\frac{\omega_{q\kappa}t}{2} \sim \lim_{q \to 0}\left\{\frac{|g_x^{q1}|^2}{\hbar^2}n_{q1}\right\}\frac{L}{v_1}t = \gamma t \quad (7)$$

with

$$\gamma = \frac{k_B T(D_c - D_v)^2(1 - 2\nu)^2}{2A\rho v_1^3 \hbar^2}. \quad (8)$$

Thus, Eq. (1) exhibits in the long-time limit an exponential decay of the polarization $p(t) \sim e^{-\gamma t}$. For an isotropic material (as assumed in our numerical calculations), we have

$$\nu = \frac{v_L^2 - 2v_T^2}{2(v_L^2 - v_T^2)}, \qquad \frac{E}{\rho} = \frac{v_T^2(3v_L^2 - 4v_T^2)}{v_L^2 - v_T^2},$$

providing a full width at half maximum of $2\hbar\gamma = 0.44$ μeV $\times T/$K for the absorption peak in agreement
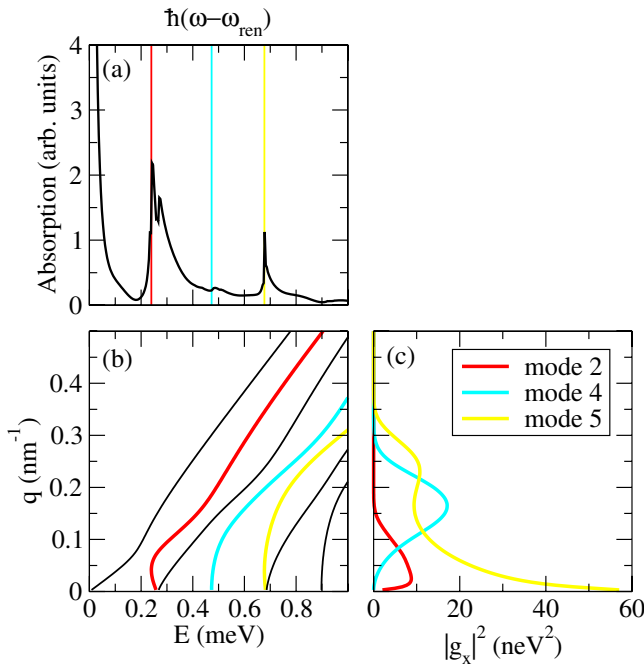

FIG. 4 (color online).   (a) Part of the absorption spectrum of the quantum dot embedded in a wire at 40 K. (b) Details of the phonon spectrum from Fig. 1 at relevant energies. (c) Magnitude of the exciton coupling for the second, fourth, and fifth mode.

with the numerical data shown above. This finite width is in contrast to the case of three-dimensional phonons [11,19,20], where the q^2 factor from the three-dimensional q integral does not allow for any contribution to the zero-phonon line.

For our calculations, we considered the phonon spectrum of ideal nanowires. For real structures, the presence of the heterostructure will modify the phonon spectrum, thus possibly changing the location of the satellite peaks. However, the qualitative nature of the acoustic branch for small wavelengths will not be affected. Thus, the broadening mechanism of the zero-phonon line should be robust, albeit a quantitative change in the width may occur.

In conclusion, we have calculated the quasi one-dimensional phonon spectrum of a GaAs nanowire and studied its impact on the excitonic absorption of an embedded quantum dot. We find pronounced satellite peaks in the absorption spectrum matching extrema in the phonon dispersion, provided that the corresponding phonon mode has a nonvanishing radial part. In addition, a finite width of the zero-phonon line of the order of $0.5\ \mu eV \times T/K$ is induced due to the wire elongation mode even for an infinite phonon lifetime. This is larger than the total width observed in quantum dots embedded in bulk material [21] for $T < 40$ K. Thus, this effect provides an essential limit for the coherence lifetime of excitons in nanowire-based quantum dots.

---

*Present address: Corrosion and Metals Research Institute, Drottning Kristinas väg 48, 114 28 Stockholm, Sweden
†Andreas.Wacker@fysik.lu.se

[1] E. Moreau, I. Robert, L. Manin, V. Thierry-Mieg, J. M. Gérard, and I. Abram, Phys. Rev. Lett. **87**, 183601 (2001).

[2] S. Kako, C. Santori, K. Hoshino, S. Götzinger, Y. Yamamoto, and Y. Arakawa, Nat. Mater. **5**, 887 (2006).

[3] K. Hennessy, A. Badolato, M. Winger, D. Gerace, M. Atatüre, S. Gulde, S. Fält, E. L. Hu, and A. Imamoglu, Nature (London) **445**, 896 (2007).

[4] R. Agarwal and C. M. Lieber, Appl. Phys. A **85**, 209 (2006).

[5] S. De Franceschi, J. A. van Dam, E. P. A. M. Bakkers, L. F. Feiner, L. Gurevich, and L. P. Kouwenhoven, Appl. Phys. Lett. **83**, 344 (2003).

[6] C. Thelander, T. Mårtensson, M. T. Björk, B. J. Ohlsson, M. W. Larsson, L. R. Wallenberg, and L. Samuelson, Appl. Phys. Lett. **83**, 2052 (2003).

[7] N. Panev, A. I. Persson, N. Sköld, and L. Samuelson, Appl. Phys. Lett. **83**, 2238 (2003).

[8] M. Borgström, V. Zwiller, E. Müller, and A. Imamoglu, Nano Lett. **5**, 1439 (2005).

[9] P. Borri, W. Langbein, S. Schneider, U. Woggon, R. L. Sellin, D. Ouyang, and D. Bimberg, Phys. Rev. Lett. **87**, 157401 (2001).

[10] D. Bimberg, M. Grundmann, and N. Ledentsov, *Quantum Dot Heterostructures* (John Wiley & Sons Ltd., New York, 1999).

[11] B. Krummheuer, V. M. Axt, and T. Kuhn, Phys. Rev. B **65**, 195313 (2002).

[12] J. Förstner, C. Weber, J. Danckwerts, and A. Knorr, Phys. Rev. Lett. **91**, 127401 (2003).

[13] J. Förstner, C. Weber, J. Danckwerts, and A. Knorr, Phys. Status Solidi B **238**, 419 (2003).

[14] J. M. Villas-Boas, S. E. Ulloa, and A. O. Govorov, Phys. Rev. Lett. **94**, 057404 (2005).

[15] A. Krügel, V. M. Axt, and T. Kuhn, Phys. Rev. B **73**, 035302 (2006).

[16] L. Besombes, K. Kheng, L. Marsal, and H. Mariette, Phys. Rev. B **63**, 155307 (2001).

[17] I. Favero, G. Cassabois, R. Ferreira, D. Darson, C. Voisin, J. Tignon, C. Delalande, G. Bastard, P. Roussignol, and J. M. Gérard, Phys. Rev. B **68**, 233301 (2003).

[18] G. D. Mahan, *Many-Particle Physics* (Plenum, New York, 2000).

[19] R. Zimmermann and E. Runge, in *Proc. 26th ICPS Edinburgh, IOP Conf. Series*, edited by A. R. Long and J. H. Davies (paper M 3.1, 2002), Vol. 171.

[20] J. Förstner, K. J. Ahn, J. Danckwerts, M. Schaarschmidt, I. Waldmüller, C. Weber, and A. Knorr, Phys. Status Solidi B **234**, 155 (2002).

[21] P. Borri, W. Langbein, U. Woggon, V. Stavarache, D. Reuter, and A. D. Wieck, Phys. Rev. B **71**, 115328 (2005).

[22] G. Ortner, D. R. Yakovlev, M. Bayer, S. Rudin, T. L. Reinecke, S. Fafard, Z. Wasilewski, and A. Forchel, Phys. Rev. B **70**, 201301 (2004).

[23] S. Rudin, T. L. Reinecke, and M. Bayer, Phys. Rev. B **74**, 161305 (2006).

[24] M. T. Björk, B. J. Ohlsson, T. Sass, A. I. Persson, C. Thelander, M. H. Magnusson, K. Deppert, L. R. Wallenberg, and L. Samuelson, Nano Lett. **2**, 87 (2002).

[25] M. W. Larsson, J. B. Wagner, M. Wallin, P. Håkansson, L. E. Fröberg, L. Samuelson, and L. R. Wallenberg, Nanotechnology **18**, 015504 (2007).

[26] M. A. Stroscio, K. W. Kim, S. Yu, and A. Ballato, J. Appl. Phys. **76**, 4670 (1994).

[27] E. A. Muljarov and R. Zimmermann, Phys. Rev. Lett. **93**, 237401 (2004).

[28] H. Haug and S. Koch, *Quantum Theory of the Optical and Electronic Properties of Semiconductors* (World Scientific, Singapore, 2004).

[29] E. A. Muljarov, T. Takagahara, and R. Zimmermann, Phys. Rev. Lett. **95**, 177405 (2005).

[30] P. Machnikowski, Phys. Rev. Lett. **96**, 140405 (2006).

[31] P. Machnikowski and L. Jacak, Phys. Rev. B **71**, 115309 (2005).

[32] E. A. Muljarov and R. Zimmermann, Phys. Rev. Lett. **98**, 187401 (2007).

[33] B. Krummheuer, V. M. Axt, and T. Kuhn, Phys. Rev. B **72**, 245336 (2005).

[34] L. D. Landau and E. M. Lifshitz, *Theory of Elasticity* (Butterworth-Heinemann, Oxford, 1986), section 25.